MULTIFRACTAL FLEXIBLY DETRENDED FLUCTUATION ANALYSIS

Rafał Rak[†], Paweł Zięba

Faculty of Mathematics and Natural Sciences, University of Rzeszów
Pigonia 1, 35-310 Rzeszów, Poland

(Received June 1, 2015; revised version received June 10, 2015)

Multifractal time series analysis is an approach that shows the possible complexity of the system. Nowadays, one of the most popular and the best methods for determining multifractal characteristics is Multifractal Detrended Fluctuation Analysis (MFDFA). However, it has a drawback. One of its core elements is detrending of the series. In the classical MFDFA, a trend is estimated by fitting a polynomial of degree m, where $m = \text{const}$. We propose that the degree m of a polynomial was not constant ($m \neq \text{const}$) and its selection was ruled by an established criterion. Taking into account the above amendment, we examine the multifractal spectra both for artificial and real-world mono- and the multifractal time series. Unlike the classical MFDFA method, obtained singularity spectra almost perfectly reflect the theoretical results, and for real time series, we observe a significant shift at the right-hand side of the spectrum.

DOI:10.5506/APhysPolB.46.1925
PACS numbers: 05.45.Df, 05.45.Tp, 89.75.–k

1. Introduction and motivation

Since people attempted to understand the surrounding reality, a lot of laws and methods have been found trying to describe this reality in a quantitative form. The major challenge for the current methods is to comprehend the behaviours and then attempt to model future states of time series, because people just have to deal with them in everyday life. The most usual records of observable quantities in nature are in the form of time series and their fractal and multifractals (nontrivial convolution of many fractals) properties have been intimately investigated [1, 2]. There is a lot of evidence that this characteristic of empirical data coming from such diverse fields as physics of turbulence flows [3], geophysics [4], astrophysics [5],

[†] Corresponding author: rafalrak@ur.edu.pl

physics of plasma [6], physiology [7], complex networks research [8] and econophysics [9] is a very important feature of so-called complex systems. It seems to be that mono-(multi-)fractal effects (typical for complex systems) may come from the nonlinear correlations as well as abundantly accompanying them the non-Gaussian heavy tails of fluctuations or both equally [10]. There are many methods that can detect the possible fractal nature of the data. For mono- and multifractal aspects, the most famous and recognized are: rescaled range (R/S) analysis [11–13], detrended fluctuation analysis (DFA) [14–16], multifractal detrended fluctuation analysis (MFDFA) [10, 14, 17–19], wavelet transform module maxima (WTMM) [19–22, 24–26], detrended moving average (DMA) [27–30] and multifractal detrending moving average (MFDMA) [31]. Nowadays, there is also a lot of activity in the area of the so-called fractal cross-correlations: multifractal detrended cross-correlation analysis MFDXA [32] and multifractal cross-correlation analysis (MFCCA) [33–35].

All the above mentioned methods of the type of $\backsim$DFA combine one expression, namely: *detrending fluctuation* which for all types of $\backsim$DFA procedures can be briefly outlined as follows. Consider time series fluctuations $x(i)$ where $i = 1, \ldots, N$. First, for a given signal $x(i)$, the profile $X(j) = \sum_{i=1}^{j} [x_i - \langle x \rangle], j = 1, \ldots, N$ is calculated ($\langle \ldots \rangle$ denotes averaging over entire time series). Second, a signal profile is divided into $M_s = \lfloor N/s \rfloor$ disjoint segments ν of length s. For each box ν, the assumed trend is estimated by fitting a polynomial P_ν^m (where $m = \text{const}$ is an order of polynomial). Next, the trend is subtracted from the data. In general, we can use a variety of values of m and the final result significantly depends on the value of m [36]. An example of detrending by different polynomials is shown in Fig. 1.

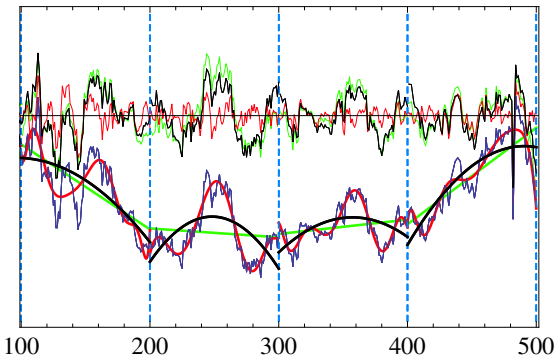

Fig. 1. An example of detrending data. The lower part shows the original time series (before detrending) and detrending polynomials P_ν^m. The upper part shows the time series detrended by different polynomials (for $m = 1$, $m = 2$ and $m = 10$).

And here comes the question: what an order m of polynomial to use? What polynomial best subtracts the trend? We cannot answer these questions unequivocally because we still do not know what 'perfectly detrended data' means and what the detrending measure is.

The MFFDFA method is tested on synthetic data (fractional Brownian motion and binomial multifractal cascade) and time series coming from real-world observables.

2. MFFDFA algorithm

As we mentioned above, Multifractal Flexibly Detrended Fluctuation Analysis (MFFDFA) has been developed on the basis the MFDFA algorithm [17], wherefore a few steps are analogous.

Step 1: Consider a signal $x(i)$, where $i = 1, \ldots, N$. For a given signal $x(i)$, the cumulative sum

$$Y(j) = \sum_{i=1}^{j} [x_i - \langle x \rangle], \qquad j = 1, \ldots, N \tag{1}$$

is calculated, where $\langle x \rangle$ denotes averaging over entire time series and N is the length of time series.

Step 2: Then the profile Y is divided into M_{s_k} partly overlapping segments ν of length s with a step $\lfloor s/k \rfloor$, where $k = 1, 2, 3, \ldots$ As a result of this modification, we get approximately k times more intervals ν of length s. Visualization of this idea is shown in Fig. 2. It is visible, that for $k = 1$, we obtain the standard MFDFA method *i.e.* segments νs non-overlapping. The minimum ($s_{\min}$) and maximum scales ($s_{\max}$) depend on the length N of the time series under study. In practice, it is reasonable to take $s_{\min} = 30$ and $s_{\max} = \lfloor N/10 \rfloor$.

Step 3: For each box, the trend is estimated by fitting all functions of a set $Q = \{f_1, f_2, \ldots, f_n\}$. Next, for each segment only one detrended function f_n is chosen of a set Q in accordance with a prescribed criterion, which is then subtracted from the signal profile. An example of detrending data using various detrending functions is shown in Fig. 3.

Step 4: For the so-detrended signal, a local variance $F^2(\nu, s)$ in each segment ν is calculated

$$F^2(\nu, s) = \frac{1}{s} \sum_{k=1}^{s} \left\{ Y((\nu - 1)s + k) - f_n^{(\nu)}(k) \right\}^2 . \tag{2}$$

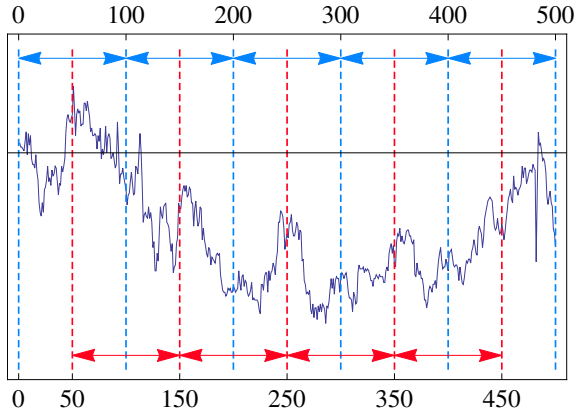

Fig. 2. An example of the division on segments ν having a length $s = 100$. The situation is shown for $k = 2$. The intervals overlap with a step $\lfloor s/k \rfloor = 50$.

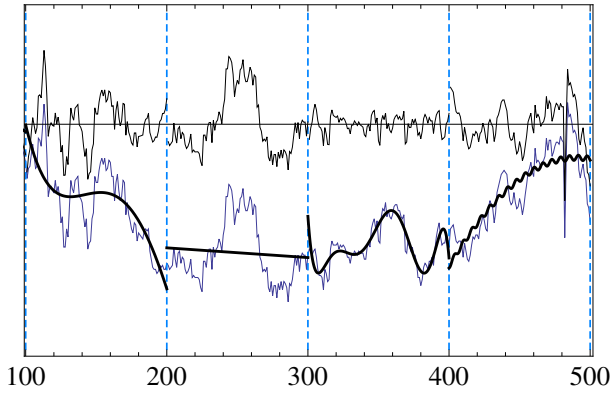

Fig. 3. An example of detrending data using different detrending functions. The lower part shows the original time series (before detrending) and detrending functions (black lines).

Finally, $F^2(\nu, s)$ averaged over all νs q^{th} order fluctuation function is derived for all possible segment lengths s:

$$F_q(s) = \left\{ \frac{1}{M_{s_k}} \sum_{\nu=1}^{M_{s_k}} \left[F^2(\nu, s) \right]^{q/2} \right\}^{1/q} , \qquad q \in \boldsymbol{R} \setminus \{0\} . \tag{3}$$

In the case when $q = 0$, the logarithmic version of Eq. (3) can be used [17]

$$F_{q=0}(s) = \frac{1}{M_{s_k}} \sum_{\nu=1}^{M_{s_k}} \ln \left| F^2(\nu, s) \right| . \tag{4}$$

Step 5: If the analysed signal is fractal, then F_q scales within some range of s according to a power law

$$F_q \sim s^{h(q)}\,, \tag{5}$$

where $h(q)$ denotes the generalized Hurst exponent. For a monofractal signal, $h(q)$ is independent of q ($h(q) = \text{const}$) and equals the Hurst exponent $h(q) = H$. On the contrary, for a multifractal time series, $h(q)$ is a decreasing function of q ($h(q) \neq \text{const}$) and the simple Hurst exponent is obtained for $q = 2$. The singularity spectrum is calculated by means of the following relation:

$$\alpha = h(q) + qh^{'}(q) \qquad \text{and} \qquad f(\alpha) = q[\alpha - h(q)] + 1\,, \tag{6}$$

where α denotes the strength of a singularity spectrum and $f(\alpha)$ is the fractal dimension of a points set with particular α. Typically, for multifractal data, the shape of the singularity spectrum is similar to a wide inverted parabola. The left and right wing of the parabola refers to the positive and negative values of q, respectively. The maximum of the spectrum is located at $\alpha(q = 0)$. For a monofractal signal, the set representing $f(\alpha)$ reduces to a single point. The wealth of multifractality is evaluated by the width of its spectrum

$$\Delta\alpha = \alpha_{\max} - \alpha_{\min}\,, \tag{7}$$

where $\alpha_{\min}$ and $\alpha_{\max}$ stand for the extreme values of α. The richer is dynamics, the larger is $\Delta\alpha$ and the more developed is the multifractal.

For all tests, in this contribution, we choose arbitrarily a set of three fitting functions $Q = \{f_1, f_2, f_3\} = \{ax^2 + bx + c,\ \ a\sin(x^2) + bx + c,\ \ ax^3 + bx + c\}$, where $\{a, b, c\}$ are constant. The criterion of function selection was based on the so-called coefficient of determination R^2. For each box ν, the function of set Q will be selected with the highest value of R.

3. Numerical tests of MFFDFA

In order to investigate the MFFDFA method, we carry out tests both for synthetic and the real-world data.

3.1. Ordinary and fractional Brownian motion

There are many different methods to create fractal time series *i.a.* based on Fourier transform filtering [37], circulant embedding of the covariance matrix [38, 39], midpoint displacement [1, 40]. In this contribution, we use Mathematica 9.0 to generate fractional Brownian motion (fBm). The long-term correlations of this Gaussian processes are completely characterized

by the Hurst exponent $H \in (0,1)$. If $H = 0.5$, time series is linearly uncorrelated and is the simplest case of a monofractal time series represented by the ordinary Brownian motion. For $0.5 < H < 1$, the data is persistent (positively correlated), which means that the signal is more likely to follow the trend. If $0 < H < 0.5$, fBm is antipersistent (negatively correlated) and consequently the signal has a tendency to change the trend direction. In our test, we have investigated fBm with different Hurst indices $H = \{0.3, 0.5, 0.9\}$. In any case, we consider, relatively short, series of length of 10,000 points. The results for each process are averaged over its 10 independent realizations in order to be statistically significant. In addition, we restrict q to $\langle -10, 10\rangle$ with a step 0.2 throughout this analysis. In Fig. 4 there is shown the comparative analysis of the standard MFDFA and modified MFDFA methods in accordance with *Step 2*. In both cases, the detrending polynomial of the order of m in the range $\langle 1, 10\rangle$ was used. It is

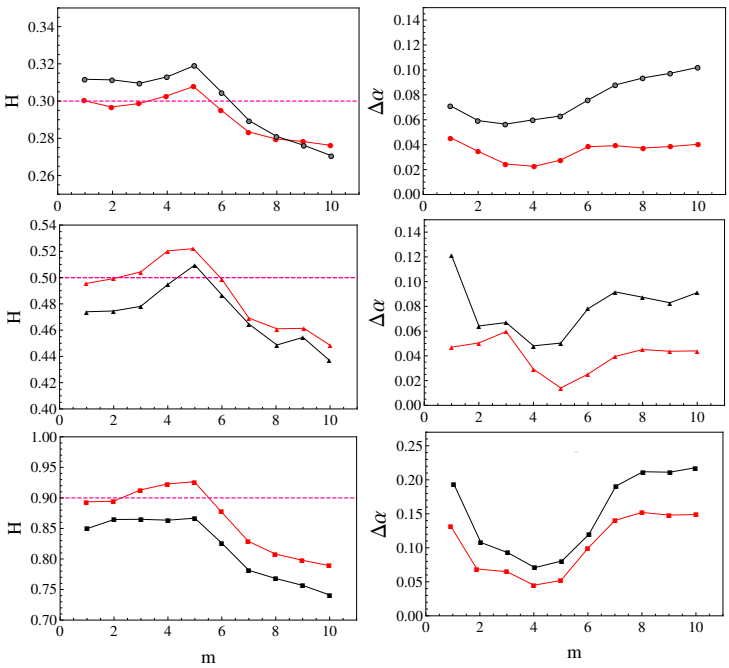

Fig. 4. Left panel: the average Hurst exponent H as a function of detrending polynomial order m. It shows the comparative analysis of standard method MFDFA (black) and modified MFDFA (grey/red) in accordance with the *Step 2* for three time series of fBm: $H = \{0.3$ (top), 0.5 (middle), 0.9 (bottom)$\}$. The right panel shows the average width of the singularity spectrum $\Delta\alpha$. The dashed horizontal lines represent the theoretical values.

clearly visible that the result strongly depends on the polynomial order m — the higher the order of a polynomial, the results more deviates from the theoretical Hurst exponent H, both for standard as well as a modified version of the MFDFA method. However, a modified version of the MFDFA leads to a much closer result theory, in particular, for polynomials of the order of $m \leq 5$. This is confirmed also by the analysis of the width of singularity spectrum $\Delta\alpha$ (right panel of Fig. 4), where the theoretical widths should be single points. In contrast to the standard MFDFA method, the widths of spectrum are much closer to zero and results for $\Delta\alpha$ are, on average, about 70 percent better for the modified MFDFA method.

The last test for monofractal time series was performed for the MFFDFA method. For the same time series as above, *i.e.* for $H = \{0.3, 0.5, 0.9\}$, we received the values $\{0.302, 0.497, 0.903\}$ respectively. What is more important, the analysis of the width of the singularity spectrum $\Delta\alpha$ indicates a much improved accuracy of MFFDFA method — for successive values of H, we received the following values of $\Delta\alpha$: $\{0.01, 0.012, 0.015\}$. The results obtained are much closer to the theoretical results, *i.e.* are closer to zero and much better than the classic methods of MFDFA. This indicates that after the introduction of the amendments in *Steps 2, 3* and *4*, the effectiveness of the method significantly increased.

3.2. Binomial multifractal cascade

A well known example in the literature of the multifractal process is a binomial multiplicative cascade [19]. This deterministic multifractal model can be defined by the following formula:

$$x_k = a^{n_{(k-1)}}(1-a)^{n_{\max}-n_{(k-1)}}\,, \tag{8}$$

where x_k is a time series of $2^{n_{\max}}$ points ($k = 1 \ldots 2^{n_{\max}}$), the parameter $a \in (0.5, 1)$ is responsible for the fractal properties and $n_{(k)}$ denotes the number of 1s in the binary representation of the index k. The fractal properties of the model are quantified by the equations of the scaling exponent and the mutifractal spectrum:

$$\tau(q) = -\frac{-\ln[a^q + (1-a)^q]}{\ln(2)}\,, \tag{9}$$

$$\alpha = -\frac{1}{\ln(2)}\frac{a^q \ln(a) + (1-a)^q \ln(1-a)}{a^q + (1-a)^q}\,, \tag{10}$$

$$f(\alpha) = -\frac{q}{\ln(2)}\frac{a^q \ln(a) + (1-a)^q \ln(1-a)}{a^q + (1-a)^q} - \frac{-\ln[a^q + (1-a)^q]}{\ln(2)}\,. \tag{11}$$

To conduct the numerical analysis, we create sets of time series of the same $n_{\max} = 17$. In this way, for a fixed value of a, we obtain a series 131 072

points long. Unlike for the Brownian processes, due to the deterministic nature of the binomial cascades under study, we create only one time series. We restrict q to $\langle -10, 10\rangle$ with a step 0.2 throughout the below analysis. In Fig. 5, there is shown the comparative analysis of the standard MFDFA method (black points) and modified MFDFA in accordance with *Step 2* (red points). Here, assume that $a = 0.65$. For these tests, we select a detrending

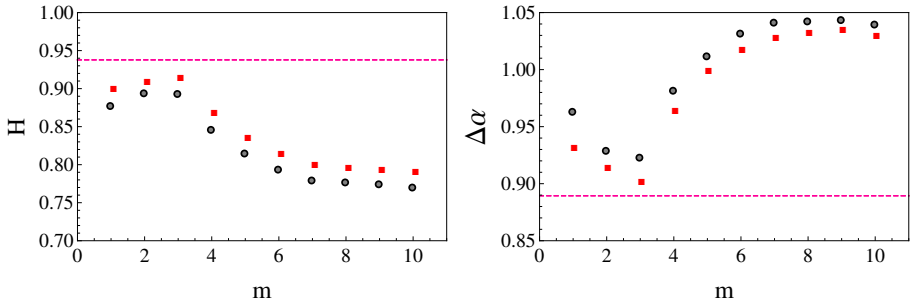

Fig. 5. Multifractal characteristics of the deterministic Binomial Cascade — the comparative analysis of the standard MFDFA method (black points) and modified MFDFA (grey/red points) in accordance with *Step 2*. Left panel: the Hurst exponent H as a function of detrending polynomial order m. Right panel: the width of the singularity spectrum $\Delta\alpha$. The dashed horizontal lines represent the theoretical values.

polynomial of the order of m in the range $\langle 1, 10\rangle$. Relatively big values of $\Delta\alpha$ confirm that the analysed time series has a multifractal nature. For all values of m, both for MFDFA and modified MFDFA, the estimated Hurst exponents are smaller than their theoretical counterparts. On the other hand, the H index increases with $1 < m \leq 3$, and for $4 \leq m < 10$, $H(m)$ is decreasing function of m. What is important, the closest results to theoretical one we observe for polynomials of the order of $m = 1, 2, 3$ and both for standard and modified MFDFA methods the polynomial of the order of 2 and 3 is the best approximation of the trend.

Another test we do for synthetic multifractal time series is a comparative analysis of the standard MFDFA and MFFDFA method. Here, we take 3 different values of $a = \{0.55, 0.65, 0.8\}$. Based on the above results, to the classical MFDFA method, we will use the detrending polynomial of the order of 3 (MFDFA3). In the case of the MFFDFA method, we use the set Q of detrending functions and criterion of their selection described at the end of Section 2. The results are shown in Fig. 6. The most distant result from a theoretical one we observe for the standard MFDFA method (top left panel). The better result was obtained for a modified version of this method (top right panel). The result, which almost perfectly reflects the theory have

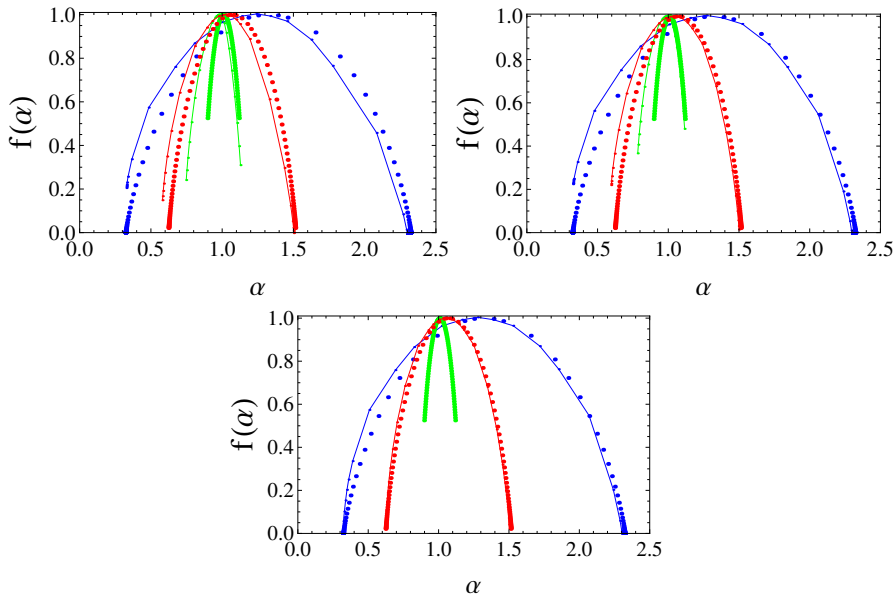

Fig. 6. Singularity spectra $f(\alpha)$ of binomial cascade for classical MFDFA and MFFDFA method. The dotted and the solid lines refer to the theoretical and the numerical results, respectively. The black, dark grey and light grey colour indicate results for various fractal parameters $a = \{0.8, 0.65, 0.55\}$, respectively. Top left panel: analysis for standard MFDFA for detrending polynomial of the order of 3. Top right panel: analysis for modified MFDFA in accordance with the *Step 2*. Bottom: analysis for MFFDFA method.

been received in the case of the MFFDFA method (Fig. 6, bottom). In the present analysis, using the MFFDFA method, the functions from the set of $Q = \{ax^2 + bx + c,\ \ a\sin(x^2) + bx + c,\ \ ax^3 + bx + c\}$ are selected on average 25%, 45%, 30%, respectively. What is important, the obtained result is a confirmation that the new MFFDFA method reflects very well not only monofractal but also multifractal nature of time series. Confirmation of this fact is the structure of the fluctuation function $F_q(s)$ shown in Fig. 7. It is clearly visible, that the fluctuation function of the new MFFDFA method is much smoother and stable than the standard MFDFA method and this, in turn, leads to a result comparable with the theory (Fig. 6, bottom, the red graph).

Furthermore, there is the asymmetric nature of the singularity spectra (see Fig. 6). Discernible is primarily left-sided asymmetry. This kind of asymmetry results from distortions/depression of the large fluctuations. We think that this asymmetry is primarily due to imperfections detrending of time series. Obviously, the asymmetry is also caused by the statistical uncertainty of the MFDFA method. These types of effects are widely explained

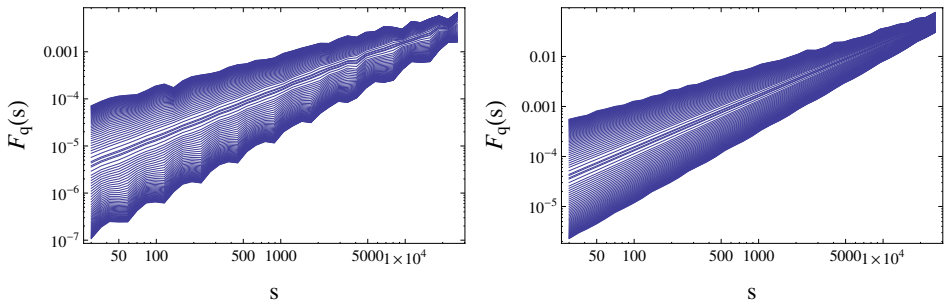

Fig. 7. Deterministic binomial cascade for $a = 0.65$. Fluctuation function $F_q(s)$ calculated for the standard MFDFA (left panel) and MFFDFA method (right panel). In both panels, the same parameters as in the top-left and bottom panel of Fig. 6 were used.

and modelled in [41]. Similar calculations (as in Fig. 6) were also carried out using a polynomial of the order of 2. We found that the singularity spectra retained asymmetric nature and their width increased slightly (according to the results in Fig. 5).

3.3. Real-world financial data

Nowadays, it is believed, that the financial markets are one of the most complex systems all over the world. The huge number of individual transactions taken together define very complex behaviour of the financial markets and lead to such characteristics of the financial data like multifractality, long memory, nonlinear correlations, the leverage effect, fat tails of financial data fluctuations, known together as the financial stylized facts [2, 42–50]. These facts led us to choose this type of data in order to test the MFDFA and MFFDFA method. We consider one-minute logarithmic price returns $r(i) = \ln(p(i+1)) - \ln(p(i))$, representing dynamics of a sample US stocks — Alcoa (AA), Walt Disney (DIS), Microsoft (MSFT) and Citigroup Inc. (C) being part of the Dow Jones Industrial index — in the period 01-01-2008–07-15-2011. Moreover, these companies were selected from different industrial sectors. As above, we focus on the widths of the singularity spectra $\Delta\alpha$ and the Hurst exponent ($H(m)$) as a function of the number of the detrending polynomial of the order of m. Results for individual companies are shown in Fig. 8. It is clearly evident that, as in the case of synthetic data, for small values of m, the parameter H is the highest and its value decreases with the increase of m. This effect is seen both for the standard MFDFA (the black symbols in Fig. 8) and its modification (the grey/red symbols). Moreover, for $m \geq 4$, the value of H is much less than 0.5, which means that analysed time series reveal high antipersitence. In this case, H calculated for $m \leq 3$ is approximately equal to 0.5, indicating uncorrelated

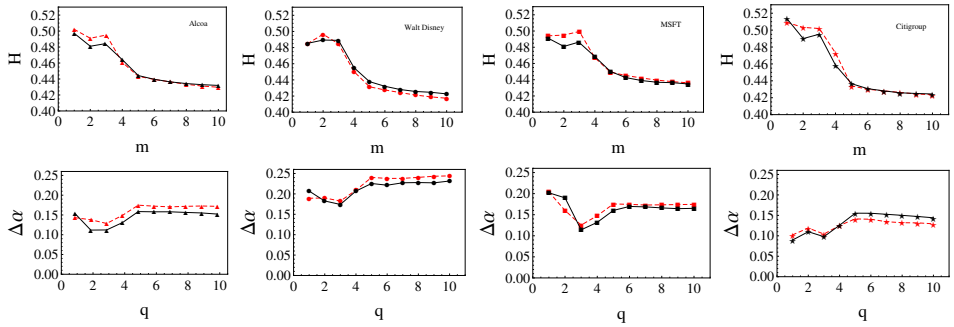

Fig. 8. Multifractal characteristics of the one-minute returns for stocks of Dow Jones Industrial index — Alcoa, Walt Disney, Microsoft and Citigroup (quoted over the period from 01-01-2008 to 07-15-2011) — the comparative analysis of the standard method MFDFA (black) and modified MFDFA (grey/red) in accordance with *Step 2*. Top panels: the Hurst exponent H as a function of detrending polynomial order m. Bottom panels: the width of the singularity spectrum $\Delta\alpha$ as a function m.

data. In Fig. 8 (bottom panels), we present the estimated $\Delta\alpha$ as a function of m. Regardless of the industry, for all listed companies in both the width of the singularity spectrum $\Delta\alpha$ and the value of H are similar in nature.

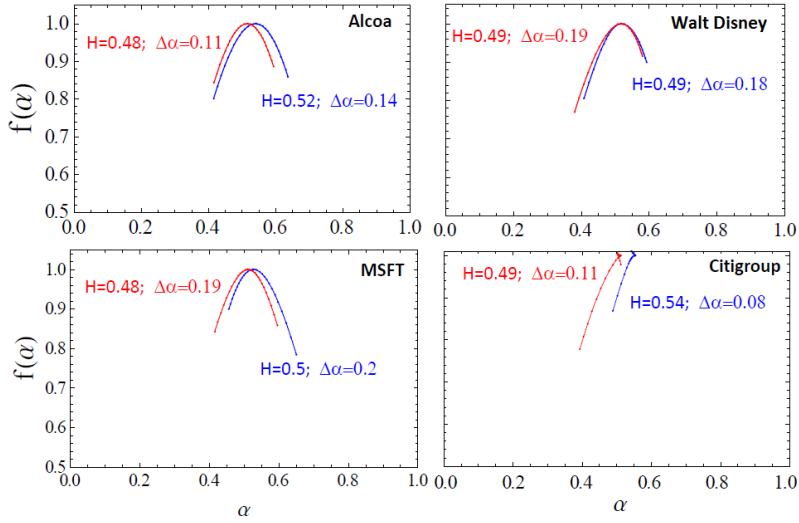

Fig. 9. Singularity spectra $f(\alpha)$ of the one-minute returns for 4 stocks of Dow Jones Industrial index quoted over the period from 01-01-2008 to 07-15-2011 — the comparative analysis of the MFDFA2 (grey/red) and MFFDFA (black/blue) methods. For each company is given the value of H and $\Delta\alpha$ for the method MFDFA2 (left side) and MFFDFA (right side).

Complementing the above considerations is the comparative analysis of the two methods (MFDFA and MFFDFA). For the standard MFDFA method (in particular MFDFA2), we used here the polynomial of the order of 2 (the most common in the literature). Using the MFFDFA method, the detrending functions from the set of Q are selected on average 21%, 40%, 39%, respectively. The results are shown in Fig. 9. It is clear that the width of all spectra for both methods are similar. Interestingly, there is noted the differences between the values of the Hurst exponent. Compared to the MFDFA method, for MFFDFA method, we observe a significant right-hand side shift of the spectrum. This effect is most visible for Citigroup — the difference between the values of H exceeds 10%. This, in turn, proves that the new MFFDFA method 'see the signal' as much more persistent.

4. Summary

In the present contribution, we generalize the classical MFDFA method and we propose a novel theoretical algorithm — Multifractal Flexibly Detrended Fluctuation Analysis (MFFDFA) — that constitutes an extension of all methods of $\backsim$DFA type. We postulate that the degree m of detrending polynomial was not constant in all segments νs ($m \neq \text{const}$). In addition, the detrending process can be made using any function. Moreover, we choose the detrended function f according to predetermined criteria. Obviously, the number and a type of functions f of set Q and the criterion for their selection is an open question.

In this paper, we test this method for synthetic data and real-world data. It turns out that the MFFDFA method (for synthetic data) leads to significantly better results. For financial data, we observe a shift of the multifractal spectra $f(\alpha)$ to the right which leads to the conclusion that the real-world data is actually more persistent than for the classical MFDFA method.

This work was partially supported by the Centre for Innovation and Transfer of Natural Sciences and Engineering Knowledge (University of Rzeszów). The calculations were done at the Academic Computer Centre CYFRONET AGH, Kraków, Poland (Zeus Supercomputer) using the Mathematica environment.

REFERENCES

[1] B.B. Mandelbrot, *The Fractal Geometry of Nature*, W.H. Freeman, New York 1983.

[2] J. Kwapień, S. Drożdż, *Phys. Rep.* **515**, 115 (2012).

[3] J.F. Muzy, E. Bacry, A. Arneodo, *Phys. Rev. Lett.* **67**, 3515 (1991).

[4] P.P. Dimitriu, E.M. Scordilis, V.G. Karacostas, *Nat. Hazards* **21**, 277 (2000); J.W. Kantelhardt *et al.*, *Physica A* **330**, 240 (2003); Y. Ashkenazy *et al.*, *Geophys. Res. Lett.* **30**, 2146 (2003); R.G. Kavasseri, R. Nagarajan, *Chaos Soliton Fract.* **24**, 165 (2005).

[5] D.W. Chappel, J. Scalo, *Astrophys. J.* **551**, 712 (2001); V.I. Abramenko, *Solar Phys.* **228**, 29 (2005); M.S. Movahed *et al.*, *J. Stat. Mech. Theory E* **0602**, P003 (2006).

[6] L.F. Burlaga, *J. Geophys. Res.* **97**, 4283 (1992); Z. Vörös *et al.*, *Ann. Geophys.* **21**, 1955 (2003).

[7] P.Ch. Ivanov *et al.*, *Nature* **399**, 461 (1999); B.J. West, M. Latka, M. Glaubic-Latka, D. Latka, *Physica A* **318**, 453 (2003); M.S. Baptista *et al.*, *Phil. Trans. R. Soc. A* **366**, 345 (2008).

[8] G. Bianconi, A.-L. Barabási, *Europhys. Lett.* **54**, 436 (2001); G. Zhu, H.J. Yang, C.Y. Yin, B.W. Li, *Phys. Rev. E* **77**, 066113 (2008).

[9] A. Fisher, L. Calvet, B. Mandelbrot, *Cowles Foundation Discussion Paper* No. **1166** (1997), Yale Research Data Center; F. Schmitt, D. Schertzer, S. Lovejoy, *Appl. Stoch. Mod. Data Anal.* **15**, 29 (1999); Z. Xu, R. Gençay, *Physica A* **323**, 578 (2003); P. Oświęcimka, J. Kwapień, S. Drożdż, *Physica A* **347**, 626 (2005).

[10] S. Drożdż, J. Kwapień, P. Oświęcimka, R. Rak, *Eur. Phys. Lett.* **88**, 60003 (2009).

[11] H.E. Hurst, *T. Am. Soc. Civ. Eng.* **116**, 770 (1951).

[12] B.B. Mandelbrot, J.W. Van Ness, *SIAM Rev.* **10**, 422 (1968).

[13] B.B. Mandelbrot, J.R. Wallis, *Water Resour. Res.* **5**, 917 (1969).

[14] C.-K. Peng *et al.*, *Phys. Rev. E* **49**, 1685 (1994).

[15] K. Hu *et al.*, *Phys. Rev. E* **64**, 011114 (2001).

[16] D. Grech, Z. Mazur, *Acta Phys. Pol. B* **36**, 2403 (2005).

[17] J.W. Kantelhardt *et al.*, *Physica A* **316**, 87 (2002).

[18] M. Ignaccolo *et al.*, *Physica A* **336**, 595 (2004).

[19] P. Oświęcimka, J. Kwapień, S. Drożdż, *Phys. Rev. E* **74**, 016103 (2006).

[20] M. Holschneider, *J. Stat. Phys.* **50**, 953 (1988).

[21] J.-F. Muzy, E. Bacry, A. Arnéodo, *Phys. Rev. Lett.* **67**, 3515 (1991).

[22] J.-F. Muzy, E. Bacry, A. Arnéodo, *J. Stat. Phys.* **70**, 635 (1993).

[23] J.-F. Muzy, E. Bacry, A. Arnéodo, *Int. J. Bifur. Chaos* **4**, 245 (1994).

[24] A. Arnéodo, E. Bacry, J.F. Muzy, *Physica A* **213**, 232 (1995).

[25] Z.R. Struzik, A. Siebes, Wavelet Transform in Similarity Paradigm I, CWI report, INS-R9802 (1998).

[26] Z.R. Struzik, A. Siebes, Wavelet Transform in Similarity Paradigm II, CWI report, INS-R9815 (1998).

[27] E. Alessio, A. Carbone, G. Castelli, V. Frappietro, *Eur. Phys. J. B* **27**, 197 (2002).

[28] A. Carbone, G. Castelli, H.E. Stanley, *Phys. Rev. E* **69**, 026105 (2004).

[29] J. Alvarez-Ramirez, E. Rodriguez, J.C. Echeverria, *Physica A* **354**, 199 (2005).

[30] L.M. Xu *et al.*, *Phys. Rev. E* **71**, 051101 (2005).

[31] G.-F. Gu, W.-X. Zhou, *Phys. Rev. E* **82**, 011136 (2010).

[32] W.-X. Zhou, *Phys. Rev. E* **77**, 066211 (2008).

[33] P. Oświęcimka *et al.*, *Phys. Rev. E* **89**, 023305 (2014).

[34] D. Horvatic, H.E. Stanley, B. Podobnik, *Europhys. Lett.* **94**, 18007 (2011).

[35] B. Podobnik, H.E. Stanley, *Phys. Rev. Lett.* **100**, 084102 (2008).

[36] P. Oświęcimka, J. Kwapień, S. Drożdż, A.Z. Górski, *Acta Phys. Pol. A* **123**, 597 (2013).

[37] R.F. Voss, *Physica D* **38**, 362 (1989).

[38] C.R. Dietrich, G.N. Newsam, *Water Resour. Res.* **29**, 2861 (1993).

[39] C.R. Dietrich, G.N. Newsam, *SIAM J. Sci. Comput.* **18**, 1088 (1997).

[40] A. Fournier, D. Fussell, L. Carpenter, *Commun. ACM* **25**, 371 (1982).

[41] S. Drożdż, P. Oświęcimka, *Phys. Rev. E* **91**, 030902(R) (2015).

[42] W.B. Arthur, *Science* **284**, 107 (1999).

[43] K. Ivanova, M. Ausloos, *Physica A* **265**, 279 (1999).

[44] J. Kwapień, P. Oświęcimka, S. Drożdż, *Physica A* **350**, 466 (2005).

[45] P. Oświęcimka *et al.*, *Acta Phys. Pol. B* **37**, 3083 (2006).

[46] R. Rak, S. Drożdż, J. Kwapień, P. Oświęcimka, *Acta Phys. Pol. B* **36**, 2459 (2005).

[47] V. Plerou *et al.*, *Phys. Rev. E* **60**, 6519 (1999).

[48] S. Drożdż *et al.*, *Acta Phys. Pol. B* **34**, 4293 (2003).

[49] X. Gabaix, P. Gopikrishnan, V. Plerou, H.E. Stanley, *Nature* **423**, 267 (2003).

[50] R. Rak, S. Drożdż, J. Kwapień, P. Oświęcimka, *Acta Phys. Pol. B* **44**, 2035 (2013).